OXFORD UNIVERSITY PRESS Toxicological Sciences

Pro-oxidant Induced DNA Damage in Human Lymphoblastoid Cells: Homeostatic Mechanisms of Genotoxic Tolerance

Journal:	*Toxicological Sciences*
Manuscript ID:	TOXSCI-11-1026.R2
Manuscript Type:	Research Article
Date Submitted by the Author:	11-Apr-2012
Complete List of Authors:	Seager, Anna; Swansea University, College of Medicine Shah, Ume-Kulsoom; Swansea University, College of Medicine Mikhail, Jane; Swansea University, College of Medicine Nelson, Bryant; National Institution of Standards and Technology, Material Measurement Laboratory- Biochemical Science Division Marquis, Bryce; National Institution of Standards and Technology, Material Measurement Laboratory- Biochemical Science Division Doak, Shareen; Swansea University, College of Medicine Johnson, George; Swansea University, College of Medicine Griffiths, Sioned; Swansea University, College of Medicine Carmichael, Paul; Unilever, Safety & Environmental Assurance Centre Scott, Sharon; Unilever, Safety & Environmental Assurance Centre Scott, Andrew; Unilever, Safety & Environmental Assurance Centre Jenkins, Gareth; Swansea University, College of Medicine
Key Words:	Genetic Toxicology, DNA repair < Genetic Toxicology, genotoxicity < Genetic Toxicology, dose-response < Risk Assessment, antioxidants < Agents, glutathione < Biotransformation and Toxicokinetics
Society of Toxicology Specialty Section Subject Area:	Molecular Biology [120]

Pro-oxidant Induced DNA Damage in Human Lymphoblastoid Cells: Homeostatic Mechanisms of Genotoxic Tolerance

Anna L Seager[*], Ume-Kulsoom Shah[*], Jane M Mikhail[*], Bryant C Nelson[†], Bryce J Marquis[†], Shareen H Doak[*], George E Johnson[*], Sioned M Griffiths[*], Paul L Carmichael[‡], Sharon J Scott[‡], Andrew D Scott[‡], Gareth J S Jenkins[*],

[*]DNA Damage Research Group, Institute of Life Science, College of Medicine, Swansea University, SA2 8PP, UK
[†]National Institute of Standards and Technology (NIST), Material Measurement Laboratory - Biochemical Science Division, 100 Bureau Drive, Gaithersburg, Maryland 20899, USA
[‡]Safety & Environmental Assurance Centre (SEAC), Unilever, Colworth Science Park, Bedford, MK44 1LQ, UK

Corresponding author: Dr Anna Seager at Swansea University, College of Medicine, ILS, Singleton Park, Swansea, SA2 8PP. email a.l.seager@swansea.ac.uk, telephone +441792295056, fax +441792602147

Running title: Pro-oxidant Genotoxicity and Thresholds levels

Abstract

Oxidative stress contributes to many disease aetiologies including ageing, neurodegeneration, and cancer, partly through DNA damage induction (genotoxicity). Understanding the interactions of free radicals with DNA is fundamental to discern the mutation risks posed. In genetic toxicology, regulatory authorities view most genotoxins to exhibit a linear relationship between dose and mutagenic response. Yet, homeostatic mechanisms exist, including DNA repair, which allow cells to tolerate low levels of genotoxic exposure. Acceptance of thresholds for genotoxicity has widespread consequences in terms of understanding cancer risk and regulating human exposure to chemicals/ drugs. Three pro-oxidant chemicals, hydrogen peroxide (H_2O_2), potassium bromate ($KBrO_3$), and menadione, were examined for low dose-response curves in human lymphoblastoid cells. DNA repair and antioxidant capacity were assessed as possible threshold mechanisms. H_2O_2 and $KBrO_3$, but not menadione, exhibited thresholded responses, containing a range of non-genotoxic low doses. Levels of the DNA glycosylase OGG1 were unchanged in response to pro-oxidant stress. DNA repair focussed gene expression arrays reported changes in *ATM* and *BRCA1*, involved in double strand break repair, in response to low dose pro-oxidant exposure, however, these alterations were not substantiated at the protein level. Determination of oxidatively induced DNA damage in H_2O_2-treated AHH-1 cells reported accumulation of thymine glycol above the genotoxic threshold. Further, the H_2O_2 dose response curve was shifted by modulating the antioxidant glutathione. Hence, observed pro-oxidant thresholds were due to protective capacities of base excision repair enzymes and antioxidants against

DNA damage, highlighting the importance of homeostatic mechanisms in "genotoxic tolerance".

Keywords

Pro-oxidants; DNA damage; reactive oxygen species; DNA repair; OGG1; antioxidants; glutathione; genotoxicology; thresholds

Introduction

Assessing the genotoxic threat of chemicals is essential in gaining a better understanding of their carcinogenic potential to reduce any deleterious effects that may be produced through occupational and recreational exposures (Doak et al., 2007; Sedelnikova et al., 2010). Traditionally, regulatory authorities utilise a linear model to assess the safety of direct-acting genotoxins, whereby a mutagenic response at high doses is extrapolated to lower doses. The so-called "single hit, single target" hypothesis, infers there is no minimal safe exposure limit for such agents (Jenkins et al., 2005). This view, however, does not account for the plethora of homeostatic mechanisms which allow mammalian cells to tolerate low levels of genotoxins. The application of a threshold mechanism in toxicology is not new, it is widely accepted that indirect-acting genotoxins, which have non-DNA targets, may exhibit a threshold mode of action (MOA) (Elhajouji et al., 2011). To date, however, the effect has been established experimentally for a limited number of DNA reactive compounds (Doak et al., 2007; Jenkins et al., 2005; Platel et al., 2009). We recently demonstrated that genotoxic thresholds induced by the alkylating agents ethyl methane sulfonate (EMS) and methyl methane sulfonate (MMS)

are due to DNA repair by the base excision repair (BER) enzyme *N*-methylpurine DNA glycosylase (MPG; GenBank ID:4350) and DNA repair protein O^6-methylguanine-DNA methyltransferase (MGMT; GenBank ID:4255), selectively removing DNA adducts at low doses but becoming saturated (or repressed) at higher doses (Doak et al., 2008; Zair et al., 2011). The acceptance of dose-response thresholds for genotoxins may have substantial regulatory implications, as well as aiding our understanding of genotoxic and neoplastic risk more fully.

An important class of DNA reactive agents present in the human environment are pro-oxidants. Mammalian cells are constantly exposed to potentially damaging reactive oxygen species (ROS) arising from multiple sources (Evans et al., 2004; Loft et al., 2008). Cellular defences exist to combat attack from ROS, including the antioxidant glutathione (GSH) and the scavenging enzyme superoxide dismutase (Forman et al., 2009). Despite this, oxidative stress and damage to cellular macromolecules can arise when the number of ROS produced exceeds the antioxidant capacity of the cell. Numerous types of DNA damage can potentially arise upon exposure to ROS, with thymine bases being the most susceptible to modification and thymine glycol representing an important thymine lesion formed after treatment by oxidising agents such as hydrogen peroxide (H_2O_2) (Basu et al., 1989).

A network of complex DNA repair pathways has thus evolved to avoid the perpetuation of such damage. Oxidised base lesions are repaired predominantly by the BER pathway. BER is mediated by damage-specific DNA glycosylases; with 8-oxoguanine DNA glycosylase (OGG1; GenBank ID:4968) repairing one of the most common forms of oxidatively generated DNA base damage, that is, 8-oxo-7,8-

dihydroguanine (8-oxoG) (Boiteux and Radicella, 2000; Wallace, 2002). The role of repair in maintaining cellular homeostasis is highlighted by reports of BER gene activation in response to genotoxic exposure (Powell et al., 2005). Further, mutation and abnormal expression of DNA repair genes, such as *ATM* (ataxia telangiectasia mutated; GenBank ID:472) and *BRCA1* (breast cancer 1, early onset; GenBank ID:672), have been directly linked with genomic instability and cancer development (Hartman and Ford, 2003; Smirnov and Cheung, 2008).

The present study focused on DNA-pro-oxidant interaction and generated genotoxic dose responses for three pro-oxidant chemicals, H_2O_2, menadione, and potassium bromate ($KBrO_3$). Two different mutagenic endpoints were assessed *in vitro* as recommended by Committee on Mutagenicity (COM); the cytokinesis block micronucleus (CBMN) assay and *HPRT* (GenBank ID:3251) forward mutation assay, examining induction of chromosomal damage and frequency of point mutations, respectively (Great Britain. Committee on Mutagenicity of Chemicals in Food, 2000). The principle aims being to analyse low-range dose-response curves, to establish the existence of possible genotoxic thresholds, and explore MOA of any observed thresholds (tolerance). Compounds were chosen due to their known capacity to generate DNA damage through differential generation of various ROS.

H_2O_2 is a physiological constituent of living cells, continually produced by a variety of cellular pathways, and has a wide range of external applications, for instance, in bleaching and in the treatment of water and sewage (Jeong et al., 2010; Naik et al., 2006). H_2O_2 is a nonradical ROS but can react via radical-mediated routes, for example, in the presence of ferrous ions undergoes Fenton's reaction to form the highly reactive

hydroxyl radical ($HO^{\bullet}$) (Pryor, 1986). Menadione is a multivitamin component and a therapeutic agent for hypothrombinemia and cancer. In the presence of flavoenzymes menadione may undergo reduction to a semiquinone; an extremely unstable compound that reacts rapidly with oxygen forming superoxide anion radical ($O_2^{\bullet -}$) and other ROS (Chung et al., 1999; Nutter et al., 1992). $KBrO_3$ has been used as a food additive primarily in bread making processes. EU countries now prohibit this application due to its proven carcinogenicity. The mechanism by which $KBrO_3$ generates damaged DNA is not fully elucidated but is believed to involve reduction of bromate by thiols such as cellular glutathione to reactive intermediates including bromine radicals ($Br^{\bullet}$) or oxides ($BrO^{\bullet}$, $BrO_2^{\bullet}$, etc.) (Ballmaier and Epe, 1995; Ballmaier and Epe, 2006).

Materials and methods

Chemicals

Buthionine sulfoximine (BSO), H_2O_2, $KBrO_3$, menadione, and N-acetylcysteine (NAC) were all purchased from Sigma (Dorset, UK). All chemical dilutions were freshly prepared from stock solutions with water.

Cell culture

The human, male, near diploid lymphoblastoid cell line AHH-1 (ATCC, Middlesex, UK) was cultured in RPMI 1640 (Life Technologies, Paisley, UK) supplemented with 1% L-glutamine (Life Technologies) and 10% donor horse serum (BDGentest, Oxford, UK) in 80-cm^2 flasks at 37ºC, 5% CO_2. The cells were maintained at a concentration of 1 to 2 x 10^5/mL. AHH-1 cells were utilised in the study as they have been widely used in genetic

toxicology and represent a versatile and reproducible system for examining genotoxic agents and the induction of gene locus mutation, including the analysis of damage response pathways and cellular defences upon free radical exposure. AHH-1 contains native CYP1a1 activity, and despite harbouring a heterozygous p53 mutation at the codon 281/282 interface within exon 8, retains the ability to undergo DNA damage induced apoptosis and has been reported to express phospho-p53 and p21 (Doak et al., 2008; Guest and Parry, 1999). Further, previous studies on thresholds have been completed utilising AHH-1, and have described stable background levels of chromosomal damage and point mutations (Doak et al., 2007; Zair et al., 2011).

Forward mutation assays

We employed the *in vitro HPRT* assay to study induced point mutations. The assay was performed as previously described (Doak et al., 2007), with the following modifications, AHH-1 cell suspensions (10mL), at 5 x 10^5/mL, were exposed to the test chemical in 80cm^3 flasks at the appropriate concentration, for 24h at 37ºC, 5% CO_2. For each dose, fifteen 96-well plates for assessing mutation frequency and another five for plating efficiency were set up. Each dose was performed in triplicate.

Micronucleus assay

Micronuclei (MN) frequency was utilised to assess the level of chromosome aberration induction. AHH-1 (10mL) suspensions of cells at 1x10^5/ mL were seeded for 24h at 37ºC, 5% CO_2. Replicate flasks (n=3, independently produced on different days) were dosed with appropriately diluted test chemical (in duplicate) for 4h, after which cells

were centrifuged, washed once in PBS, and re-suspended in 10mL fresh media containing 6µg/mL cytochalasin B for one cell cycle (22h). Treated cells were harvested, re-suspended in 10mL of hypotonic solution (0.56% KCl), and centrifuged immediately. Cell suspension was re-suspended in fixative 1 (methanol: acetic acid: 0.9% NaCl (5:1:6 parts)) and centrifuged after a 10min incubation period. Cells were transferred to fixative 2 (methanol: acetic acid (5:1 parts)) for a 10min incubation, centrifuged, washed 4 times, and maintained in the final fixative 2-wash at 4ºC for 16h. Fixed cells were centrifuged, and 100µL dropped onto polished, fixed, and hydrated slides, stained with DAPI (4', 6-diamido-2-phenylindole; 0.15µg/ mL final concentration), and viewed under a Carl Zeiss AxioImager fluorescent microscope. Slides were scored utilising the Metafer4 software version 3.5 (MetaSystems, Altlussheim, Germany). An optimal scoring criterion was achieved from the development of specific classifiers adjusted to accommodate the particular lymphoblast cell line (AHH-1), and to identify binucleate cells containing MN. The criteria for identifying micronuclei were as previously described (Fenech, 2007). A minimum of two thousand binucleated cells were scored per replicate, and each dose was performed in triplicate (an average of 6000 binucleates per dose).

RNA isolation and gene expression analysis

Following exposure to the test pro-oxidants for 0h, 2h, 4h, and 24h time-points, total cellular RNA was isolated from AHH-1 cells followed by DNase treatment using the RNeasy mini kit (Qiagen, West Sussex, UK), and TURBO DNA-free kit (Ambion, Huntingdon, UK), respectively, according to the manufacturer's instructions. Quantitative PCR of mRNA was performed as a one-step reaction, where the entire reaction from

cDNA synthesis to real-time PCR amplification is performed in a single well, on a MyIQ™5 cycler optics module (BioRad, Hertfordshire, UK). Commercially available Taqman® Gene Expression Assays and human endogenous controls were purchased from Applied Biosystems (UK); supplied as pre-mixed primers and FAM/ MGB probe. To perform one-step real time PCR, *OGG1* target gene (Hs00213454_m1*) and *HPRT* reference gene (4333768) probes were used in conjunction with QuantiFast Probe RT-PCR kit (Qiagen). Approximately 0.2µg RNA was used for cDNA synthesis and PCR in a reaction volume of 20µL, containing 10µl of 2x QuantiFast Probe RT-PCR Master Mix, 0.4µl QuantiFast RT Mix, and 1µl of Taqman probe mix (primers and probe at final concentrations of 900nM and 250nM, respectively). The following PCR reaction protocol was used: initially cDNA production occurred for 1 cycle at 50°C for 10min followed by 95°C for 5min. Subsequently, PCR was initiated for 40 cycles of 95°C for 10s and 61°C for 30s. Reactions were performed in triplicate and the level of gene expression is reported as the ratio between the mRNA level of the target gene and the HPRT reference gene using the relative standard curve method.

Western Blot analysis

Following exposure to the test pro-oxidants for 0h, 2h, 4h, and 24h time-points, total cellular protein was isolated from AHH-1 cells. Cells were pelleted by centrifugation, washed in ice-cold PBS, then lysed in RIPA buffer (Sigma), supplemented with protease inhibitor cocktail (Sigma) at 4°C for 5min. Cells were further lysed by agitation and centrifugation, and the cell pellet discarded. Protein extracts (30ng) of AHH1 cells were resolved on 10% SDS-PAGE (Sodium dodecyl sulphate-polyacrylamide gel

electrophoresis) at 120V, transferred onto polyvinylidene difluoride (PVDF) membranes (BioRad), and blocked for 1h at room temperature with 5% Bovine serum albumin (BSA) in TBS-T (20mM Tris (pH 7.6), 125mM NaCl, 0.1% (v/v) Tween20). Membranes were incubated with monoclonal mouse anti-OGG1 (Sigma), polyclonal rabbit anti-beta tubulin (AbCam, Cambridge, UK), monoclonal rabbit anti-ATM (Cell Signaling Technology, Massachusets, USA), polyclonal rabbit anti-BRCA1 (Cell Signaling Technology), or monoclonal rabbit anti-beta actin (Cell Signalling Technology) antibodies overnight at 4ºC. Following washing (4 × 5 min in TBS/T), membranes were incubated with appropriate horseradish peroxidase (HRP) conjugated secondary antibodies (AbCam). Protein bands were detected using the Immuno-Star Western C chemiluminescence kit (BioRad). Membranes were visualised using the Bio-Rad Chemidoc XRS and average band density analysis was performed using Quantity One version 4.6.3 (BioRad).

Human DNA repair PCR arrays

To assess the role of a wider range of DNA repair enzymes in the observed non-linear damage responses to pro-oxidants, gene expression PCR arrays tailored for DNA repair were utilised. AHH-1 cells were treated with specific doses above and below confirmed threshold inflection points, which were 5µM and 25µM H_2O_2, 0.2mM and 0.8mM $KBrO_3$, and 0.5mM and 3.5mM menadione, for 4h and the RNA was extracted. RNA (1.6µg) from each sample was reverse transcribed into cDNA using the RT² First Strand Kit (Qiagen). Gene expression was performed utilising Human DNA Repair RT² Profiler™ PCR Arrays (PAHS-042A) and 2X SABiosciences RT² qPCR Master Mix (Qiagen) and

MyiQ real-time PCR Platform (BioRad) according to the manufacturer's instructions. Gene expression was normalised using five housekeeping genes within the array and quantified using the ΔΔCt method by accessing the PCR Array Data Analysis Web Portal http://www.SABiosciences.com/pcrarraydataanalysis.php.

Gas Chromatography/Mass Spectrometry (GC/MS) Determination of Oxidatively Induced DNA Damage

GC/MS with isotope dilution was used to determine the absolute levels of five different oxidatively modified bases: 8-oxoG, thymine glycol (TG), 5-hydroxy-5-methylhydantoin (5-OH-5-MeHyd), 2,6-diamino-4-hydroxy-5-formamidopyrimidine (FAPyG) and 4,6-diamino-5-formamidopyrimidine (FAPyA). AHH-1 cells were seeded for 24h and treated with 0, 5 μM/ mL and 25 μM/ mL H_2O_2 for 4h. Following washing, DNA was extracted from the treated cells using the DNeasy Blood & Tissue Kit (Qiagen). The DNA was precipitated and GC/MS analyses were performed as previously described (Dizdaroglu, 1985; Jaruga et al., 2008).

Alteration of cellular GSH levels

In order to modulate GSH levels prior to measuring pro-oxidant induced MN, GSH was either supplemented or depleted. AHH-1 (10mL) suspensions of cells at $1x10^5$/ mL were seeded for 24h at 37ºC, 5% CO_2. Cells were dosed with 2mM NAC to promote glutathione levels and increase cellular antioxidant status, or 0.5mM BSO an inhibitor of glutathione synthesis, for 24h prior to pro-oxidant treatment and CBMN assay (as

previously described). The levels of GSH in treated cells were estimated utilising the Glutathione Assay kit (Sigma) according to the manufacturer's instructions.

Statistical analysis

For the genotoxicity data and DNA adduct data, a one-way Analysis of Variance (ANOVA), followed by a Dunnett's posthoc test, was used to determine if any of the treatment doses were significantly different from the zero dose, except when cells were pre-treated with BSO or NAC, where a *T*-test was employed. The hockey stick modelling of apparent thresholds was carried out using software, kindly provided by Lutz and Lutz (Lutz and Lutz, 2009) and implemented in the R package. A *T*-test was performed to establish any differences between relative protein and mRNA expression of *OGG1* after pro-oxidant treatments at the different time points analysed. Independent sample *T* test was utilised to analyse differences in normalised protein levels of ATM and BRCA1 after treatment with H_2O_2 (0-25μM) or $KBrO_3$ (0-0.8mM).

Results

The cytokinesis blocked micronucleus (CBMN) and *HPRT* forward mutation assays were used to assess the induction of chromosomal aberration (MN formation) and frequency of point mutations, respectively, after exposure of AHH-1 lymphoblastoid cells to low concentrations of the oxidising agents. The range of concentrations used was determined following initial dose setting experiments analysing genotoxicity and assessment of cytotoxicity utilising relative population doubling (RPD) calculations in satellite cultures (data not shown). To ensure any observed genetic damage was not due

to cytotoxicity related mechanisms, only those concentrations leading to more than 50% cell viability were analysed (data not shown). Investigations into the MOA behind these threshold responses involved analysis of levels of DNA repair enzymes involved in the repair of oxidative damage, assessment of the levels of oxidatively modified bases in exposed DNA, and analysis of the effect of antioxidant status on the dose-response curves to chromosome damage. To ensure cellular exposure to ROS was occurring at low doses of pro-oxidants, oxidation of the non-fluorescent probe 2′,7′-dichlorofluorescein-diacetate (DCFH-DA) to the fluorochrome 2,7-dichlorofluorescein (DCF) was used as an index to quantify the overall level of intracellular ROS produced by 0 to 100μM H_2O_2 (Supplementary file S1).

Gene mutation induction

The *HPRT* forward mutation assay was used here to investigate the mutagenic activity of H_2O_2, $KBrO_3$, and menadione. All three pro-oxidants demonstrated a range of low doses with minimal levels of mutation induction in AHH-1 human lymphoblastoid cells as compared to solvent control data (Fig. 1). The first statistically significant increase in mutation frequency above background levels (lowest observed effect level; LOEL) was 18μM for H_2O_2 (p= 0.004), 0.5mM for $KBrO_3$ (p= 0.004), and 2.9μM for menadione (p= 0.001) utilising one-way ANOVA, followed by a Dunnett's posthoc test. Further analysis of these results applying a "hockey-stick model" developed by Lutz and Lutz (2009) rejected linearity of each dose response curve, whilst supporting a threshold model (p< 0.05) and showed that H_2O_2 had an inflection point (or threshold dose) at 7.3μM with lower confidence interval (CI) of 2.04μM; $KBrO_3$ an inflection point of

0.18mM with lower CI of 0.08mM; and menadione an inflection point of 1.89µM with lower CI of 0.76mM (Fig 1.) (Lutz and Lutz, 2009).

Chromosomal damage induction

The dose-response relationships, with respect to the induction of chromosome aberrations, obtained after pro-oxidant treatments with H_2O_2, $KBrO_3$, and menadione are illustrated in Figure 2. LOEL concentrations of 25µM (p= 0.03), 0.6mM (p= 0.007), and 2.9µM (p= 0.036) were identified for exogenous treatment with H_2O_2, $KBrO_3$, and menadione, respectively. Subsequent increases in concentration above each LOEL produced a progressive rise in cellular DNA damage, as detected by a higher incidence of MN. Hockey stick statistical modelling of the data using the Lutz approach rejected a linear fit to the dose response curves and confirmed an inflection point (threshold value) of 10.88µM with lower CI of 5.93µM and 0.35mM with lower CI of 0.22mM, for H_2O_2 and $KBrO_3$, respectively. The dose-response curve for menadione, despite indicating a non-linear response for the induction of genotoxic damage, favoured a linear model and did not achieve significance when hockey stick modelling was performed on the data.

Base excision repair (BER) glycosylase cellular levels

In order to examine the protective mechanisms behind the genotoxic tolerance to low doses of pro-oxidants shown here, we focussed firstly on the role of DNA repair. Previous work on thresholded responses for the alkylating agents has demonstrated upregulation of the DNA repair enzymes *MPG* and *MGMT* by EMS and MMS, respectively, at doses below the threshold (Doak et al., 2008; Zair et al., 2011). Since, 8-

oxoG is a major DNA lesion formed as a consequence of ROS exposure and 8-oxoG in DNA is primarily repaired by the DNA glycosylase OGG1, the mRNA and protein levels of this enzyme were measured in response to specific pro-oxidant treatment (in this case H_2O_2). *OGG1* expression levels in treated and untreated AHH-1 lymphoblastoid cells, measured by real-time RT-PCR, are represented in Figure 3A. No significant modulation in *OGG1* expression in response to H_2O_2 treatment (0-50μM) was observed at any of the time points (0-24h) studied. OGG1 protein levels in AHH-1 cells following oxidative insult were also analysed by Western blotting and normalized to beta-tubulin expression (Fig. 3B). Similarly to mRNA levels, treatment with H_2O_2 (0-50μM) had no detectable effect on the amount of OGG1 protein recovered from nuclear extracts at any of the treatment periods (0-24h) monitored, comparable results were observed for treatment with 1mM $KBrO_3$ (results not shown).

Human DNA repair PCR arrays

To investigate the effects of pro-oxidant treatment on a wider range of DNA repair genes within this interesting thresholded region, treated cells were analysed using DNA repair-directed PCR gene expression arrays. Since only H_2O_2 and $KBrO_3$ showed thresholds for both point mutation and chromosome damage, these studies concentrated on these two pro-oxidants. The PCR expression arrays focus on a selected panel of eighty-four genes involved in the base-excision, nucleotide excision, mismatch, double-strand break, and other DNA repair processes (Supplementary file S2). Numerous fold changes in expression, compared to untreated control cells, were observed above and below the threshold doses (Table 1). *ATM* for example (an important gene involved in the

signalling response to DNA damage), showed unchanged expression levels at concentrations below the threshold doses, but was observed to be 2.13 fold (H_2O_2) and 4.0 fold ($KBrO_3$) downregulated above the threshold dose for chromosome damage induction, suggestive of a relatively higher degree of damage recognition below the threshold. The cancer susceptibility gene *BRCA1*, involved in the repair of DNA double strand breaks (DSBs), was upregulated by 2.39 and 2.04 fold (H_2O_2 and $KBrO_3$, respectively) at concentrations below but not above the thresholds for chromosomal damage in both chemicals. H_2O_2 treated cells also exhibited a 2.69 fold increase in expression of *APEX1* (APEX nuclease (multifunctional DNA repair enzyme) 1; GenBank ID:328) at a concentration below, but not above, the threshold dose, indicative of a role for BER in minimising chromosome damage at low H_2O_2 doses. Further, the BER DNA glycosylase *MUTYH* (mutY homolog (E.coli); GenBank ID:4595), which catalyses the removal of adenine bases from the DNA backbone at sites where adenine is inappropriately paired with guanine, cytosine, or 8-oxoG, was downregulated by 2.17 fold after exposure to 0.8mM $KBrO_3$.

Relative levels of DNA damage response proteins

To further investigate the gene expression changes observed during the PCR gene array experiments, and to ascertain whether such expression changes were consistently observed at the protein level, the amount of ATM and BRCA1 protein recovered from nuclear extracts after pro-oxidant treatment was determined in AHH-1 cells. Cells were dosed with H_2O_2 and $KBrO_3$ at concentrations above and below the thresholds for chromosome damage induction, and relative protein levels were deduced by Western

blotting via the examination of band intensities of ATM or BRCA1 normalised to beta-actin loading controls (Fig. 4). Unlike the alterations in *ATM* and *BRCA1* mRNA expression observed following treatment with concentrations of H_2O_2 above (25μM) or below (5μM) the threshold, no significant threshold-dependent differences in the levels of these DNA repair proteins were detected (Fig. 4A). Treatment with 0.2mM $KBrO_3$ (below the threshold) appeared to induce an increase in protein levels of both ATM and BRCA1 (Fig. 4B), which then decreased at 0.8mM $KBrO_3$ (above the threshold) to levels comparable to untreated samples, however these differences were not deemed significant by independent sample *T* test.

GC/MS Determination of Oxidatively Induced DNA Damage

Four out of the five modified bases were detected in the AHH-1 DNA extracts (Fig. 5). The FAPyA lesion was not detectable in either the control or the H_2O_2-treated samples, most likely due to the low amount (~ 30μg) of extracted DNA/sample available for MS analysis. Of the four detected lesions, the levels of the 8-oxoG, FAPyG and 5-OH-5-MeHyd lesions in the H_2O_2-treated samples were not significantly different from the background levels in the control samples. The TG lesion, however, was found to be significantly (p= 0.0259) increased in the 25μM H_2O_2-treated sample (Fig. 5D), in comparison to the TG background level in the control samples. The level of TG in the 5μM H_2O_2-treated sample was not significantly different from the TG levels in the controls. The accumulation of TG in the 25μM H_2O_2-treated sample could potentially have biological relevance as TG is a cytotoxic lesion that is a known block to DNA polymerase.

Impact of GSH on pro-oxidant induced DNA damage

GSH is the principal non-protein thiol involved in the antioxidant cellular defence, playing a critical role in protecting cells from oxidative damage and the toxicity of xenobiotic electrophiles, as well as maintaining redox homeostasis (Forman et al., 2009). To elucidate the function of antioxidants in the observed genotoxic threshold effects described above, intra-cellular levels of GSH were modified and the shapes of the resultant dose-response curves for H_2O_2, with respect to chromosomal damage, were assessed. AHH-1 cells were pre-treated with BSO (0.5mM), a specific GSH synthesis inhibitor, or NAC (2.0mM), a GSH precursor, for 24h and the effects on H_2O_2 -induced DNA damage were determined by the CBMN assay (Fig. 6). BSO pre-treatment altered the shape of the H_2O_2 dose-response curve significantly from a thresholded curve to a linear dose-response which saturates at higher doses. BSO pre-treatment reduced the first dose to induce a statistically significant increase in genetic damage from 18μM to 8μM (p= 0.0008), which indicates that GSH depletion by BSO (confirmed utilising a GSH assay) reduces protection against oxidatively induced DNA damage, at low dose treatments. Furthermore, statistically significant increases in micronuclei frequency were observed in BSO pre-treated cells at 10μM (p< 0.001) and 12μM (p< 0.01) H_2O_2 as compared to cells without pre-treatment. In contrast, NAC pre-treated cells had significantly lower levels of micronuclei induction at 18μM (p< 0.001) and 25μM (p< 0.01) H_2O_2, as compared to H_2O_2 cells without pre-treatment suggestive of a protective effect of enhanced GSH status.

Discussion

Elevated cellular levels of ROS can imbalance homeostasis and create oxidative stress, and chronic exposure to this stress can cause permanent genomic changes. Accumulation of oxidative lesions has been associated with ageing and a host of human diseases including cancer, chronic inflammation, atherosclerosis, and neurodegenerative diseases such as Alzheimer's disease(Sedelnikova et al., 2010). The use of oxidative DNA damage measurements in populations may have important implications for human health risk assessment, distinguish relevant environmental exposures, and predict frequency of disease (Hatt et al., 2008; Loft et al., 2008).

Traditionally, characterisation of DNA-reactive agents has involved the assumption of a linear relationship between genotoxin exposure and induction of mutagenic modifications (Henderson et al., 2000). This view, however, does not account for homeostatic mechanisms that potentially counteract DNA damage induced after genotoxic exposure. Knowledge of the dose-response relationship of a given chemical is paramount; if a threshold exists, safe levels can be calculated, if there is a linear dose-response, there are no safe exposure levels. This can have economic implications; impacting the availability and use of certain compounds.

To investigate the biological significance of low-dose exposures, a robust analysis of mutation and chromosomal damage induction was performed with the DNA-reactive compounds H_2O_2, $KBrO_3$, and menadione. All three pro-oxidants displayed a range of low doses with no statistically significant increase above background levels of DNA damage induction. Objective analysis of the data employing "hockey stick" statistical modelling demonstrated inflection (threshold) points for each of the dose relationships,

except for chromosomal damage induction in menadione, which conformed to a linear model. Menadione, may thus, be considered a non-thresholded compound overall. The linear relationship of damage induction observed after menadione exposure may be explained by the reported production of a high frequency of DNA strand scission by the compound mediated by $HO^{\bullet}$, that may be too extensive for the repair machinery to correct, even at low doses (Nutter et al., 1992). Although DNA strand breaks occur after exposure to H_2O_2 and $KBrO_3$, other oxidative lesions such as 8-oxoG and TG occur preferentially (Cadet et al., 2010; Kawanishi and Murata, 2006).

Thresholds were reported at lower concentrations (1.5 to 2 fold) for point mutations than for MN induction, which may be explained by the higher probability of a single oxidative lesion formation yielding a base substitution, compared to a DSB arising from multiple clustered lesions. Indeed, abortive BER processing of radical damage can form DSBs when the position of lesions are closely opposed on the two strands (Wallace, 2002).

Several mechanisms may be responsible for contributing to genotoxic thresholds in response to ROS, however, DNA repair is likely to be the primary mode of defence. Repair pathways may well successfully remove newly formed adducts at low doses, and if the rate of lesion repair is faster than its rate of formation, a no observable effect limit (NOEL) will result. We have previously noted that thresholds for alkylating agents (EMS and MMS) are accompanied by increases in the expression of DNA repair genes *MGMT* and *MPG* (Doak et al., 2008; Zair et al., 2011).

A well studied biomarker of oxidative damage, and a key repairable DNA lesion induced by the pro-oxidants studied, is 8-oxoG. 8-oxoG is a premutagenic DNA lesion

due to its propensity to mispair with adenine, generate errors in replication, and G:C to T:A transversions. It is a substrate for the BER pathway, initiated by the OGG1 enzyme (Boiteux and Radicella, 2000; Nishimura, 2002). To investigate the potential of OGG1 as a thresholded mode of action (MOA), gene and protein expression of OGG1 were examined. No modulation in OGG1 levels was observed in response to oxidative stress; which is in agreement with other studies (Mistry and Herbert, 2003; Saitoh et al., 2001). Furthermore, *OGG1* has been described as a "house keeping" gene with a constant level of expression throughout the cell cycle (Dhenaut et al., 2000). Basal, not inducible, expression of *OGG1* therefore, may play a role in the maintenance of homeostasis in the presence of low levels of pro-oxidants.

A lack of OGG1 induction may reflect the redundancy that exists between BER glycosylases, and indeed between other pathways to repair oxidative lesions. Further investigation into the responses of other DNA repair genes to pro-oxidant stress was needed, and to fulfil this requirement the gene expression profile of eighty-four key DNA repair enzymes was compared at doses above and below the thresholds of chromosome damage induction observed for H_2O_2 and $KBrO_3$ (S2). For most of the nine genes with altered expression there was no clear pattern for the two chemicals and therefore it is difficult to propose a direct mechanistic link in which a threshold level of exposure determines a switch in the expression of the DNA damage response program. Despite this, two repair genes showed interesting results; *ATM*, a central component of the DSB repair pathway in mammalian cells, was downregulated above the threshold doses for damage induction and *BRCA1*, a nuclear phosphoprotein that plays a role in maintaining

genomic stability, was upregulated below the threshold doses for damage induction in both H_2O_2 and $KBrO_3$.

Analysis of protein levels of these DNA damage response genes following exposure to pro-oxidants, however, did not substantiate the PCR array findings, and no significant alterations in the protein levels of ATM or BRCA1 were observed above or below the genotoxic thresholds. Thus, although DSB may occur under oxidative stress conditions, such as when ROS induced DNA damage interferes with either DNA replication or transcription such as during the processing of bulky DNA adducts such as FAPyG produced from ring opening of guanine upon exposure to $HO^{\bullet}$, it is not involved in the MOA of genotoxic thresholds observed for pro-oxidants. In agreement with this conclusion, in the present study, FAPyG lesions were observed at similar levels at doses above and below the H_2O_2 threshold and thus appear to be repaired effectively or are not formed upon exposure to low doses. In contrast, TG levels were significantly higher in 25μM H_2O_2-, but not in 5μM H_2O_2-treated samples, versus untreated controls.

TG is the most common thymine lesion found after treatment by oxidising agents and exerts significant distortion on the duplex DNA molecule, blocking replication. There are instances, however, whereby DNA polymerases can by-pass TG and a low level of misincorporation of guanine opposite thymine glycol occurs, giving rise to mutation (Wallace, 2002). The presence of higher levels of TG above the threshold suggests a role for this lesion, and BER in the observed genotoxic thresholds. The BER glycosylases NEIL1 (nei endonuclease VIII-like 1; GenBank ID:79661) and NTHL1 (nth endonuclease III-like 1; GenBank ID: 4913) may successfully remove TG at low doses but above the threshold the glycosylases are ‘saturated’, lesions start to escape repair,

becoming fixed permanent defects, and subsequent increases in dose result in a more linear increase in damage. Alternatively, formation of TG may be reduced below the threshold due to lower exposure to ROS.

DNA repair represents but one tier of protection against oxidatively generated DNA damage present in multicellular organisms. Antioxidants may also contribute to the above described thresholds. Alteration of the antioxidant status of cells via the manipulation of GSH levels, transformed the shape of the dose-response curve of H_2O_2 induced chromosomal damage. For example, inhibition of GSH by BSO altered the shape of the curve from a non-linear threshold to a more linear response, and reduced the lowest dose to induce a statistically significant increase in genetic damage from 25μM to 8μM H_2O_2. Furthermore, boosting GSH levels with NAC shifted the dose response to the right, with treated cells showing significantly lower levels of MN induction at 18μM and 25μM H_2O_2, as compared to H_2O_2 cells without pre-treatment. Such effects suggest a causal role for GSH in the genotoxic thresholds of pro-oxidants, competing with DNA to accept electrons from ROS, removing their oxidative capacity and potential to create mutagenic lesions. Altering the redox status *in vitro* by increasing the levels of antioxidants has beneficial, protective effects against pro-oxidant agents.

Although it is difficult to extrapolate from the *in vitro* data described here to an *in vivo* setting, the existence of a NOEL implies at least a pragmatic threshold for carcinogenicity of H_2O_2 and $KBrO_3$. Genotoxic tolerance to low levels of pro-oxidant chemicals appears to be due, in part, to basal BER DNA repair plus the protective capacity of antioxidants against DNA damage. The abundance of repair pathways and significant redundancy achieved by overlapping substrates in maintaining REDOX

homeostasis suggest that the persistence of oxidative DNA damage is extremely detrimental to cells. Theoretically, as genetic alterations do not arise at very low doses, the risk of carcinogenesis (and also several degenerative chronic diseases) is unlikely to occur after exposure to concentrations below the LOEL, as no biologically significant effects are observed experimentally. This outcome has implications on the numerous uses of pro-oxidant chemicals including as cosmetic bleaches, as cancer treatment agents and in food production. Furthermore, the present study strengthens the evidence of the existence of thresholds for direct-acting genotoxins.

Supplementary data

Intracellular ROS production by H_2O_2 was measured using the oxidation-sensitive fluoroprobe 2′,7′-dichlorofluorescin diacetate (DCFH-DA, Invitrogen molecular probes). DCFH-DA assay is based on the principle that upon cellular internalisation, the DA portion of the hydrophobic dye is cleaved by esterases. The resulting DCFH is oxidised to its highly fluorescent product DCF by cellular oxidants, thereby indicating the level of intracellular ROS. DCFH-DA was dissolved in DMSO to a concentration of 1M and was further diluted to the appropriate concentration with Hepes-buffered (20 mM) Hanks balanced salt solution with glucose (5mM) (pH 7.4). A 2µM aliquot of DCFH-DA was added to the wells of a 96-well plate previously loaded with AHH-1 cells and 0 to 100µM H_2O_2, and fluorescence was measured over 30min with fluorescence excitation and emission at 480 and 520 nm, respectively. The supplementary graph (S1) shows the relative fluorescence after exposure of AHH-1 cells to 0 to 100µM H_2O_2 (mean of triplicate experiments). There were non-significant increases in the quantity of ROS

production measured over background (untreated) levels after exposure to doses within the range of the threshold of H_2O_2. ROS production was observed at significantly higher levels than background samples after exposure to 15μM of H_2O_2, a dose higher than the threshold observed within the study, by One-way ANOVA, followed by Dunnett's post hoc analysis (p= 0.032).

Complete analysis of the DNA repair PCR expression arrays detailing the expression levels of eighty-four human repair genes after exposure to H_2O_2 and $KBrO_3$ doses above and below the threshold inflection point (output from hockey stick statistical modelling) is supplied as a supplementary table (S2).

Funding

This work was supported by Unilever PLC. URL:http://www.unilever.co.uk/.

NIST Disclaimer

Certain commercial equipment, instruments and materials are identified in this paper to specify an experimental procedure as completely as possible. In no case does the identification of particular equipment or materials imply a recommendation or endorsement by the National Institute of Standards and Technology nor does it imply that the materials, instruments, or equipment are necessarily the best available for the purpose.

References

Ballmaier, D., and Epe, B. (1995). Oxidative DNA damage induced by potassium bromate under cell-free conditions and in mammalian cells. Carcinogenesis *16*, 335-342.

Ballmaier, D., and Epe, B. (2006). DNA damage by bromate: mechanism and consequences. Toxicology *221*, 166-171.

Basu, A. K., Loechler, E. L., Leadon, S. A., and Essigmann, J. M. (1989). Genetic effects of thymine glycol: site-specific mutagenesis and molecular modeling studies. Proc Natl Acad Sci U S A *86*, 7677-7681.

Boiteux, S., and Radicella, J. P. (2000). The human OGG1 gene: structure, functions, and its implication in the process of carcinogenesis. Arch Biochem Biophys *377*, 1-8.

Cadet, J., Douki, T., and Ravanat, J. L. (2010). Oxidatively generated base damage to cellular DNA. Free Radic Biol Med *49*, 9-21.

Chung, S. H., Chung, S. M., Lee, J. Y., Kim, S. R., Park, K. S., and Chung, J. H. (1999). The biological significance of non-enzymatic reaction of menadione with plasma thiols: enhancement of menadione-induced cytotoxicity to platelets by the presence of blood plasma. FEBS Lett *449*, 235-240.

Dhenaut, A., Boiteux, S., and Radicella, J. P. (2000). Characterization of the hOGG1 promoter and its expression during the cell cycle. Mutat Res *461*, 109-118.

Dizdaroglu, M. (1985). Application of capillary gas chromatography-mass spectrometry to chemical characterization of radiation-induced base damage of DNA: implications for assessing DNA repair processes. Anal Biochem *144*, 593-603.

Doak, S. H., Brusehafer, K., Dudley, E., Quick, E., Johnson, G., Newton, R. P., and Jenkins, G. J. (2008). No-observed effect levels are associated with up-regulation of MGMT following MMS exposure. Mutat Res *648*, 9-14.

Doak, S. H., Jenkins, G. J., Johnson, G. E., Quick, E., Parry, E. M., and Parry, J. M. (2007). Mechanistic influences for mutation induction curves after exposure to DNA-reactive carcinogens. Cancer Res *67*, 3904-3911.

Elhajouji, A., Lukamowicz, M., Cammerer, Z., and Kirsch-Volders, M. (2011). Potential thresholds for genotoxic effects by micronucleus scoring. Mutagenesis *26*, 199-204.

Evans, M. D., Dizdaroglu, M., and Cooke, M. S. (2004). Oxidative DNA damage and disease: induction, repair and significance. Mutat Res *567*, 1-61.

Fenech, M. (2007). Cytokinesis-block micronucleus cytome assay. Nat Protoc *2*, 1084-1104.

Forman, H. J., Zhang, H., and Rinna, A. (2009). Glutathione: overview of its protective roles, measurement, and biosynthesis. Mol Aspects Med *30*, 1-12.

Great Britain. Committee on Mutagenicity of Chemicals in Food, C. P. a. t. E. (2000). Guidance on a strategy for testing of chemicals for mutagenicity ([Great Britain], Committee on Mutagenicity of Chemicals in Food, Consumer Products and the Environment).

Guest, R. D., and Parry, J. M. (1999). P53 integrity in the genetically engineered mammalian cell lines AHH-1 and MCL-5. Mutat Res *423*, 39-46.

Hartman, A. R., and Ford, J. M. (2003). BRCA1 and p53: compensatory roles in DNA repair. J Mol Med *81*, 700-707.

Hatt, L., Loft, S., Risom, L., Moller, P., Sorensen, M., Raaschou-Nielsen, O., Overvad, K., Tjonneland, A., and Vogel, U. (2008). OGG1 expression and OGG1 Ser326Cys polymorphism and risk of lung cancer in a prospective study. Mutat Res *639*, 45-54.

Henderson, L., Albertini, S., and Aardema, M. (2000). Thresholds in genotoxicity responses. Mutat Res *464*, 123-128.

Jaruga, P., Kirkali, G., and Dizdaroglu, M. (2008). Measurement of formamidopyrimidines in DNA. Free Radic Biol Med *45*, 1601-1609.

Jenkins, G. J., Doak, S. H., Johnson, G. E., Quick, E., Waters, E. M., and Parry, J. M. (2005). Do dose response thresholds exist for genotoxic alkylating agents? Mutagenesis *20*, 389-398.

Jeong, M. S., Lee, C. M., Jeong, W. J., Kim, S. J., and Lee, K. Y. (2010). Significant damage of the skin and hair following hair bleaching. J Dermatol *37*, 882-887.

Kawanishi, S., and Murata, M. (2006). Mechanism of DNA damage induced by bromate differs from general types of oxidative stress. Toxicology *221*, 172-178.

Loft, S., Hogh Danielsen, P., Mikkelsen, L., Risom, L., Forchhammer, L., and Moller, P. (2008). Biomarkers of oxidative damage to DNA and repair. Biochem Soc Trans *36*, 1071-1076.

Lutz, W. K., and Lutz, R. W. (2009). Statistical model to estimate a threshold dose and its confidence limits for the analysis of sublinear dose-response relationships, exemplified for mutagenicity data. Mutat Res *678*, 118-122.

Mistry, P., and Herbert, K. E. (2003). Modulation of hOGG1 DNA repair enzyme in human cultured cells in response to pro-oxidant and antioxidant challenge. Free Radic Biol Med *35*, 397-405.

Naik, S., Tredwin, C. J., and Scully, C. (2006). Hydrogen peroxide tooth-whitening (bleaching): review of safety in relation to possible carcinogenesis. Oral Oncol *42*, 668-674.

Nishimura, S. (2002). Involvement of mammalian OGG1(MMH) in excision of the 8-hydroxyguanine residue in DNA. Free Radic Biol Med *32*, 813-821.

Nutter, L. M., Ngo, E. O., Fisher, G. R., and Gutierrez, P. L. (1992). DNA strand scission and free radical production in menadione-treated cells. Correlation with cytotoxicity and role of NADPH quinone acceptor oxidoreductase. J Biol Chem *267*, 2474-2479.

Platel, A., Nesslany, F., Gervais, V., and Marzin, D. (2009). Study of oxidative DNA damage in TK6 human lymphoblastoid cells by use of the in vitro micronucleus test: Determination of No-Observed-Effect Levels. Mutat Res *678*, 30-37.

Powell, C. L., Swenberg, J. A., and Rusyn, I. (2005). Expression of base excision DNA repair genes as a biomarker of oxidative DNA damage. Cancer Lett *229*, 1-11.

Pryor, W. A. (1986). Oxy-radicals and related species: their formation, lifetimes, and reactions. Annu Rev Physiol *48*, 657-667.

Saitoh, T., Shinmura, K., Yamaguchi, S., Tani, M., Seki, S., Murakami, H., Nojima, Y., and Yokota, J. (2001). Enhancement of OGG1 protein AP lyase activity by increase of APEX protein. Mutat Res *486*, 31-40.

Sedelnikova, O. A., Redon, C. E., Dickey, J. S., Nakamura, A. J., Georgakilas, A. G., and Bonner, W. M. (2010). Role of oxidatively induced DNA lesions in human pathogenesis. Mutat Res *704*, 152-159.

Smirnov, D. A., and Cheung, V. G. (2008). ATM gene mutations result in both recessive and dominant expression phenotypes of genes and microRNAs. Am J Hum Genet *83*, 243-253.

Wallace, S. S. (2002). Biological consequences of free radical-damaged DNA bases. Free Radic Biol Med *33*, 1-14.

Zair, Z. M., Jenkins, G. J., Doak, S. H., Singh, R., Brown, K., and Johnson, G. E. (2011). N-methylpurine DNA glycosylase plays a pivotal role in the threshold response of ethyl methanesulfonate-induced chromosome damage. Toxicol Sci *119*, 346-358.

Table 1. Alterations in DNA repair gene expression above and below the threshold for chromosome damage induction.

	Fold change in gene expression			
Gene symbol	**5μM H_2O_2**	**25μM H_2O_2**	**0.2mM $KBrO_3$**	**0.8mM $KBrO_3$**
APEX1	2.69	1.14	n/a	2.57
ATM	0.52	-0.47	1.08	-0.25
BRCA1	2.39	1.71	2.04	1.89
ERCC4	0.55	0.74	0.66	-0.5
FEN1	-0.46	0.83	0.61	-0.44
LIG3	0.53	0.7	0.62	-0.47
MUTYH	0.54	0.74	0.62	-0.46
PNKP	-0.41	0.71	0.53	-0.34
TOP3B	0.51	0.79	0.55	-0.43

Figure legends

Figure 1. Gene mutation frequency in response to pro- oxidants.

Dose-response relationships of hydrogen peroxide (H_2O_2), potassium bromate ($KBrO_3$), and menadione, in the AHH-1 cell line with respect to *HPRT* gene mutation frequency. Hockey stick statistical modelling analysis has been applied to each data set to calculate the inflection point (IP), probability for non- linearity (*p*) and *Y*- intercept. *(A)* H_2O_2, threshold, IP= 7.28µM, lowerIP/CI= 2.04µM, *Y*= 1.95, and *p*= 0.038. (*B*) $KBrO_3$, threshold, IP= 0.18mM, lowerIP/CI= 0.08mM, *Y*= 6.11, and *p*= 0.004. (*C*) Menadione, threshold, IP= 1.89µM, lowerIP/CI= 0.76µM, *Y*= 5.05, and *p*= 0.004.

Figure 2. Chromosomal damage in response to pro- oxidants.

Dose-response relationships of hydrogen peroxide (H_2O_2), potassium bromate ($KBrO_3$), and menadione, in the AHH-1 cell line with respect to micronucleus frequency. Hockey stick statistical modelling analysis has been applied to each data set to calculate the inflection point (IP), probability for non- linearity (*p*) and *Y*- intercept. (*A*) H_2O_2, threshold, IP= 10.88µM, lower IP/CI= 5.93µM, *Y*= 1.32, and *p*= 0.023. (*B*) $KBrO_3$, threshold, IP= 0.35mM, lower IP/CI= 0.22mM, *Y*= 1.05, and *p*= 0.002. (*C*) Menadione, linear, and *p*= 0.35. *Mn/Bn%*: percentage of binucleated cells containing one or more micronuclei.

Figure 3. Effect of hydrogen peroxide on OGG1 levels.

(A) Effect of hydrogen peroxide (H_2O_2) on *OGG1* expression in AHH-1 cells. Cells were treated with 0- 50µM of H_2O_2 and total RNA extracted between 0 and 24h. Levels of

OGG1 mRNA were assessed by real time RT PCR. Values were normalized to levels of the constitutively expressed housekeeping gene, *HPRT*, and represent the mean (± SD) fold change from control levels at each time point. Each data point represents three independent measurements. *(B)* Western blot of OGG1 protein and loading control B-tubulin in AHH-1 cells following treatment with 25µM H_2O_2 for 0, 2, 4, and 24h; *L*: ladder.

Figure 4. Effects of pro-oxidants on protein levels of ATM and BRCA1.

(A) Effect of hydrogen peroxide (H_2O_2) on ATM and BRCA1 protein levels recovered form AHH-1 cells treated for 4 hours with concentrations above (25µM) and below (5µM) the genotoxic threshold for DNA damage induction. *(B)* Effect of potassium bromate ($KBrO_3$) on ATM and BRCA1 protein levels recovered form AHH-1 cells treated for 4 hours with concentrations above (0.2mM) and below (0.8mM) the genotoxic threshold for DNA damage induction. *Normalised protein level*: Relative protein concentration calculated using membrane band intensities normalised to beta-actin loading control band intensities. *Bars*: standard deviation.

Figure 5. Determination of oxidatively induced DNA damage in hydrogen peroxide-treated AHH-1 cells.

(A) Accumulation of 8-oxo-7,8-dihydroguanine (8-oxoG) in relation to exposure dose, *(B)* Accumulation of 2,6-diamino-4-hydroxy-5-formamidopyrimidine (FAPyG) in relation to exposure dose, *(C)* Accumulation of 5-hydroxy-5-methylhydantoin (5-OH-5-MeHyd) in relation to exposure dose, *(D)* Accumulation of thymine glycol (TG) in

relation to exposure dose. *: ($p < 0.05$) indicates statistically significant result compared to the control samples using one-way Analysis of Variance (ANOVA) followed by Dunnett's multiple comparison test. All data points represent the mean of ≥ 4 independent measurements. Uncertainties are standard deviations.

Figure 6. Pro-oxidant dose response following alteration of cellular glutathione antioxidant levels.

Effect of BSO (0.5mM) or NAC (2.0mM) pre-treatment on the frequency of hydrogen peroxide (H_2O_2) induced micronuclei in AHH-1 cells; *: At 8 μM H_2O_2, first significant increase in micronuclei (MN) frequency above the control in BSO pre- treated cells (p= 0.0008) as determined by *T*-test. &: At 10uM H_2O_2, BSO pre- treated cells demonstrated a statistically significant increase in percentage MN as compared to non pre-treated and NAC pre- treated cells ($p<0.001$ and $p< 0.05$, respectively); **: At 12μM H_2O_2, BSO pre- treated cells showed a statistically significant elevation in MN as compared to non pre- treated cells ($p<0.01$); $: At 18uM H_2O_2, first statistically significant increase in MN frequency above the control in non pre- treated cells ($p<0.0001$); also, non pre-treated cells exhibited statistically significant higher levels of MN to NAC pre-treated cells ($p<0.001$); ***: At 25uM H_2O_2, non pre-treated cells had statistically significant higher levels of micronuclei than NAC pre-treated cells ($p<0.01$). *Mn/Bn%*: percentage of binucleated cells containing one or more micronuclei.

Supplementary Figure S1. Effect of hydrogen peroxide (H_2O_2) on DCFH-DA fluorescence.

Intracellular ROS production by H_2O_2 was measured using the oxidation-sensitive fluoroprobe 2′,7′-dichlorofluorescin diacetate (DCFH-DA). * ($p< 0.05$) and ** ($p<0.005$) indicates statistically significant result compared to the control zero samples using one-way Analysis of Variance (ANOVA) followed by Dunnett's multiple comparison test. Each bar represents the mean of three independent measurements. Uncertainties are standard deviations.

Supplementary Figure S2. Effect of pro-oxidants on the expression levels of human repair genes.

Table depicting the complete analysis of the DNA repair PCR expression arrays detailing expression levels of eighty-four human repair genes after exposure to 5uM- and 25µM-H_2O_2 and 0.2mM- and 0.8mM-$KBrO_3$ doses (above and below the threshold inflection point, respectively) relative to control (untreated) samples.

Abbreviations

5-OH-5-MeHyd= 5-hydroxy-5-methylhydantoin

8-oxoG= 8-oxo-7,8-dihydroguanine

ATM= ataxia telangiectasia mutated

Bn= binuclieated cells

BRCA1= breast cancer 1

BSA= bovine serum albumin

BSO= buthionine sulfoximine

CBMN= cytokinesis block micronucleus assay

CI= confidence interval

CO_2= carbon dioxide

DAPI= 4',6-diamido-2-phenylindole

DCFH-DA= 2′,7′-dichlorofluorescin diacetate

EMS= ethyl methane sulphonate

FAPyA= 4,6-diamino-5-formamidopyrimidine

FAPyG= 2,6-diamino-4-hydroxy-5-formamidopyrimidine

GSH= glutathione

h= hours

H_2O_2= hydrogen peroxide

HAT= hypoxanthine-aminopterin-thymidine

HPRT= hypoxanthine phosphoribosyltransferase

HO•= hydroxyl radical

HRP= horse radish peroxidise

IP= inflection point

$KBrO_3$= potassium bromate

KCl= potassium chloride

LOEL= low observed effect level

MGMT= O^6-methylguanine-DNA methyltransferase

MPG= *N*-methylpurine-DNA glycosylase

MMS= methyl methane sulphonate

MN= micronuclei

MOA= modes of action

NAC= N-acetylcysteine

NaCl= sodium chloride

$^{\bullet}NO$= nitric oxide

$^{\bullet}NO_2$= nitrogen dioxide radical

NOEL= no observed effect level

$O_2^{\bullet-}$= superoxide anion radical

OGG1= 8-oxoguanine DNA glycosylase 1

P= probability

PAGE= polyacrylamide gel electrophoresis

PBS= phosphate buffered saline

PVDF= polyvinylidene difluoride

ROS= reactive oxygen species

RPD= relative population doubling

SDS= sodium dodecyl sulphate

TBS= Tris-buffered saline

TG= thymine glycol

TRIS= Tris(hydroxymethyl)aminomethane

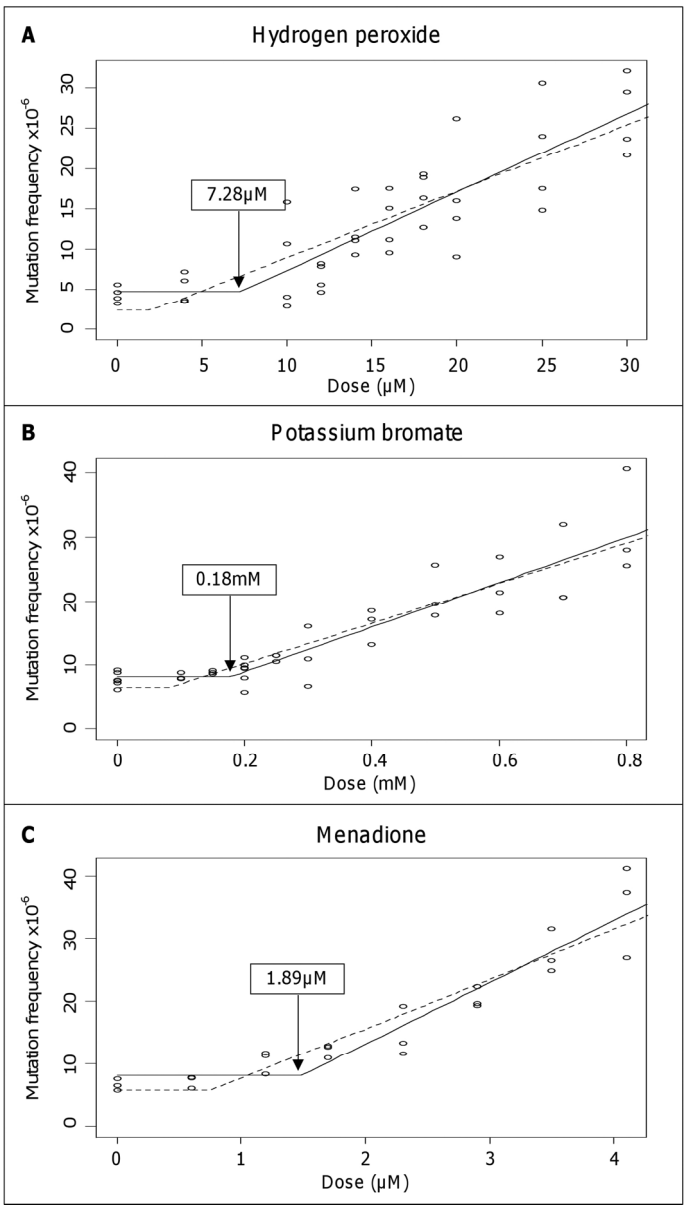

Figure 1. Gene mutation frequency in response to pro- oxidants.
Dose-response relationships of hydrogen peroxide (H2O2), potassium bromate (KBrO3), and menadione, in the AHH-1 cell line with respect to HPRT gene mutation frequency. Hockey stick statistical modelling analysis has been applied to each data set to calculate the inflection point (IP), probability for non- linearity (p) and Y- intercept. (A) H2O2, threshold, IP= 7.28μM, lowerIP/CI= 2.04μM, Y= 1.95, and p= 0.038. (B) KBrO3, threshold, IP= 0.18mM, lowerIP/CI= 0.08mM, Y= 6.11, and p= 0.004. (C) Menadione, threshold, IP= 1.89μM, lowerIP/CI= 0.76μM, Y= 5.05, and p= 0.004.
156x274mm (300 x 300 DPI)

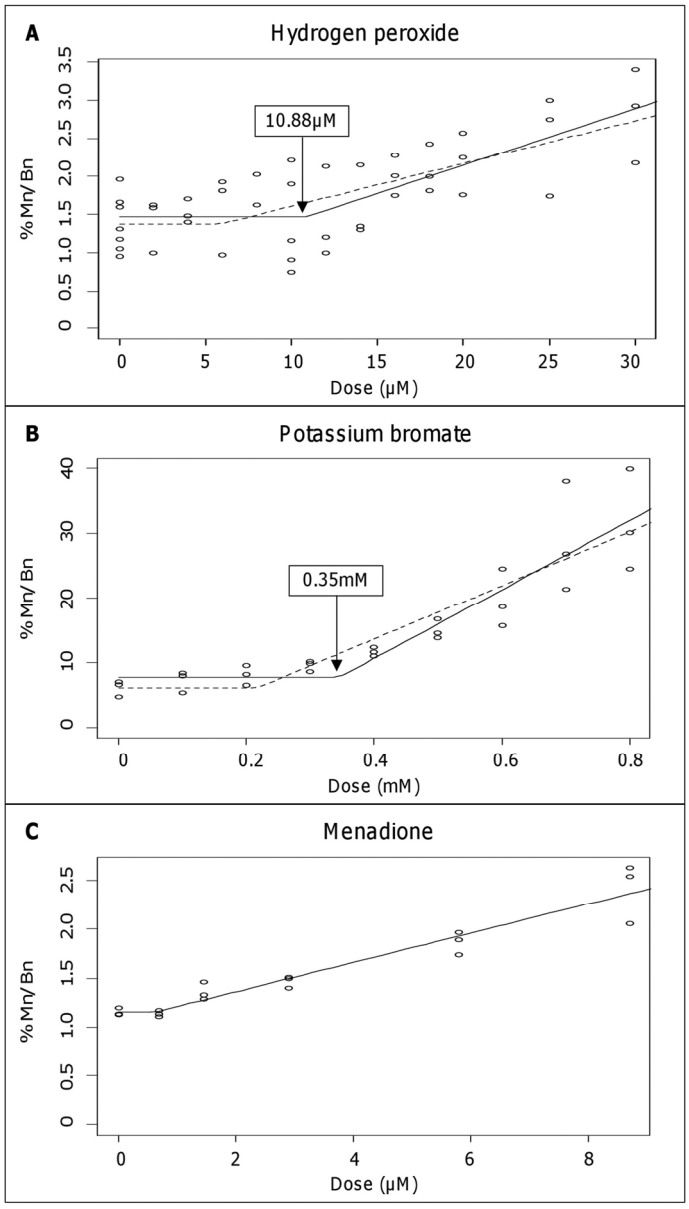

Figure 2. Chromosomal damage in response to pro- oxidants.
Dose-response relationships of hydrogen peroxide (H2O2), potassium bromate (KBrO3), and menadione, in the AHH-1 cell line with respect to micronucleus frequency. Hockey stick statistical modelling analysis has been applied to each data set to calculate the inflection point (IP), probability for non- linearity (p) and Y-intercept. (A) H2O2, threshold, IP= 10.88μM, lower IP/CI= 5.93μM, Y= 1.32, and p= 0.023. (B) KBrO3, threshold, IP= 0.35mM, lower IP/CI= 0.22mM, Y= 1.05, and p= 0.002. (C) Menadione, linear, and p= 0.35. Mn/Bn%: percentage of binucleated cells containing one or more micronuclei.
155x272mm (300 x 300 DPI)

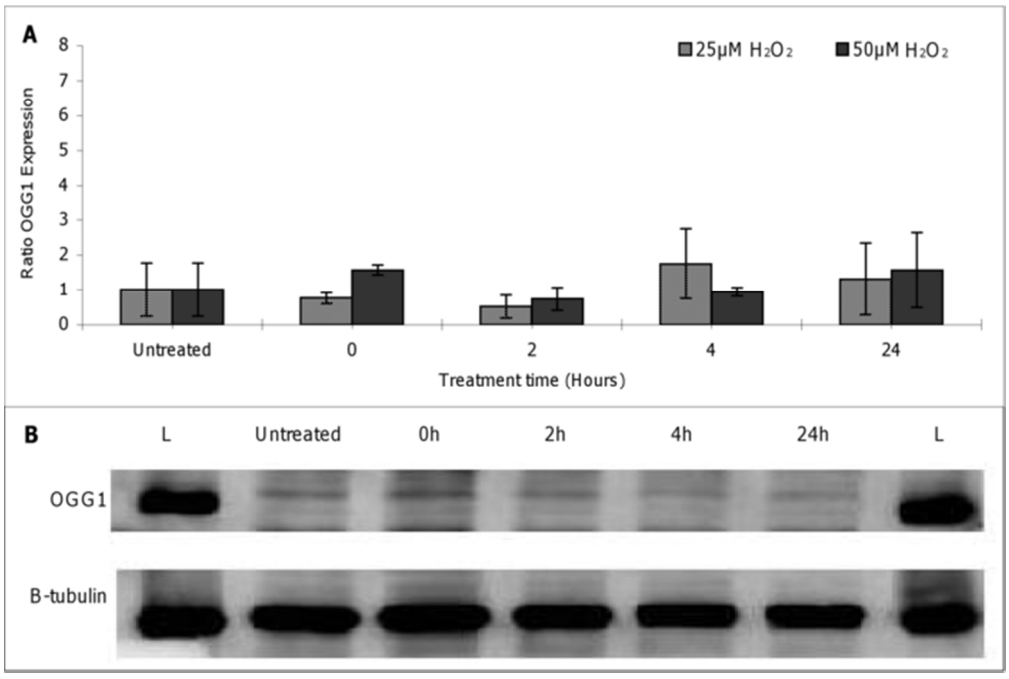

Figure 3. Effect of hydrogen peroxide on OGG1 levels.
(A) Effect of hydrogen peroxide (H2O2) on OGG1 expression in AHH-1 cells. Cells were treated with 0- 50μM of H2O2 and total RNA extracted between 0 and 24h. Levels of OGG1 mRNA were assessed by real time RT PCR. Values were normalized to levels of the constitutively expressed housekeeping gene, HPRT, and represent the mean (± SD) fold change from control levels at each time point. Each data point represents three independent measurements. (B) Western blot of OGG1 protein and loading control B-tubulin in AHH-1 cells following treatment with 25μM H2O2 for 0, 2, 4, and 24h; L: ladder.
59x39mm (300 x 300 DPI)

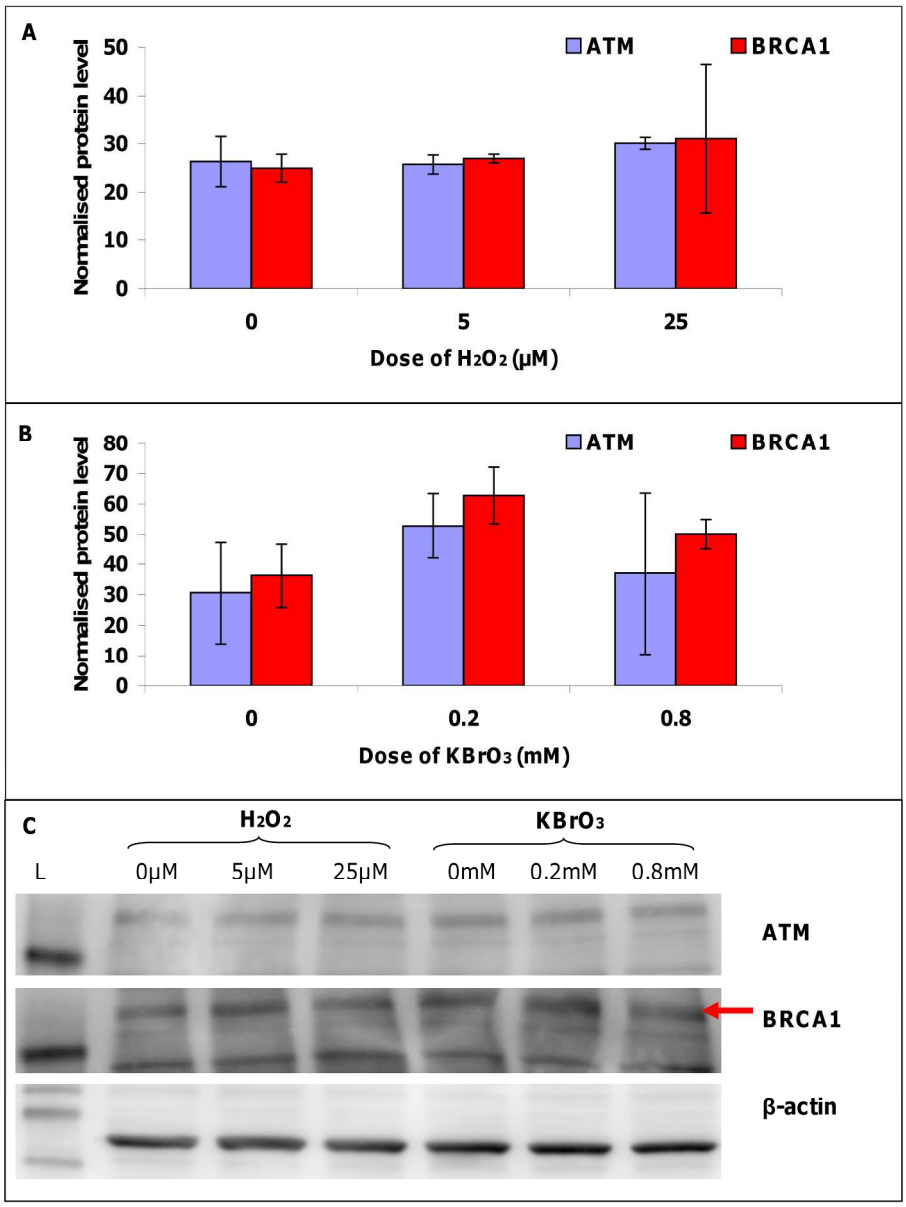

Figure 4. Effects of pro-oxidants on protein levels of ATM and BRCA1.
(A) Effect of hydrogen peroxide (H2O2) on ATM and BRCA1 protein levels recovered form AHH-1 cells treated for 4 hours with concentrations above (25μM) and below (5μM) the genotoxic threshold for DNA damage induction. (B) Effect of potassium bromate (KBrO3) on ATM and BRCA1 protein levels recovered form AHH-1 cells treated for 4 hours with concentrations above (0.2mM) and below (0.8mM) the genotoxic threshold for DNA damage induction. Normalised protein level: Relative protein concentration calculated using membrane band intensities normalised to beta-actin loading control band intensities. Bars: standard deviation.
209x279mm (300 x 300 DPI)

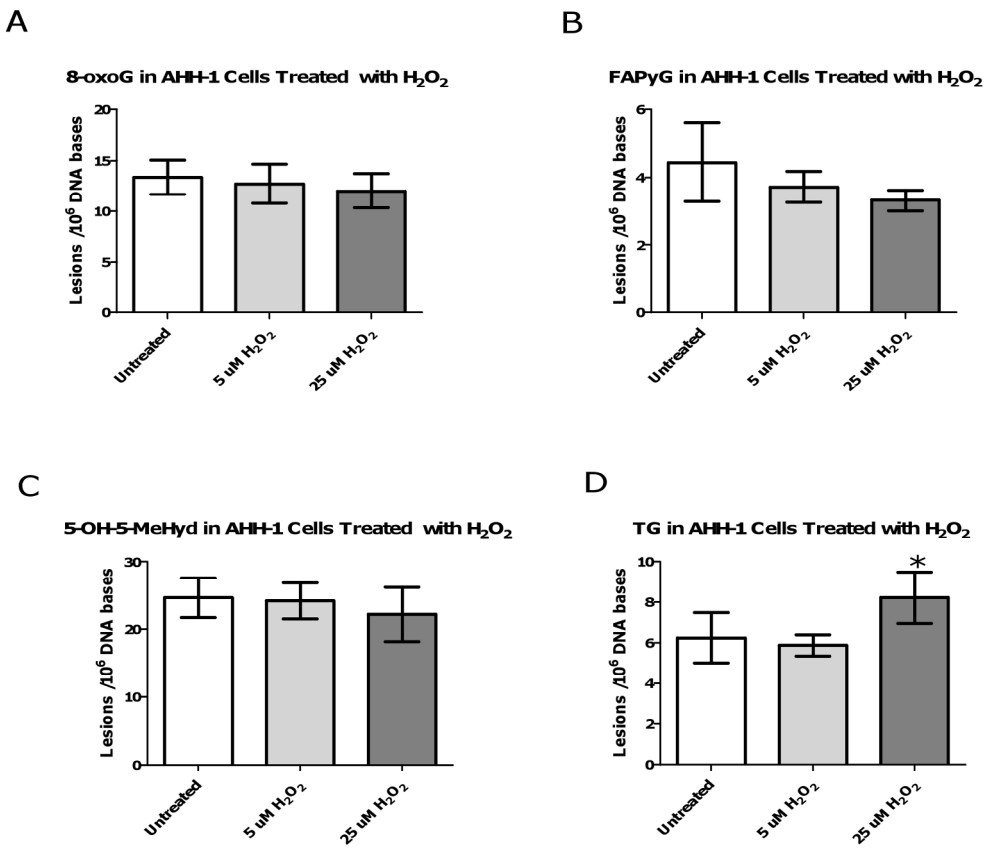

Figure 5. Determination of oxidatively induced DNA damage in hydrogen peroxide-treated AHH-1 cells. (A) Accumulation of 8-oxo-7,8-dihydroguanine (8-oxoG) in relation to exposure dose, (B) Accumulation of 2,6-diamino-4-hydroxy-5-formamidopyrimidine (FAPyG) in relation to exposure dose, (C) Accumulation of 5-hydroxy-5-methylhydantoin (5-OH-5-MeHyd) in relation to exposure dose, (D) Accumulation of thymine glycol (TG) in relation to exposure dose. *: ($p < 0.05$) indicates statistically significant result compared to the control samples using one-way Analysis of Variance (ANOVA) followed by Dunnett's multiple comparison test. All data points represent the mean of ≥ 4 independent measurements. Uncertainties are standard deviations.
187x161mm (300 x 300 DPI)

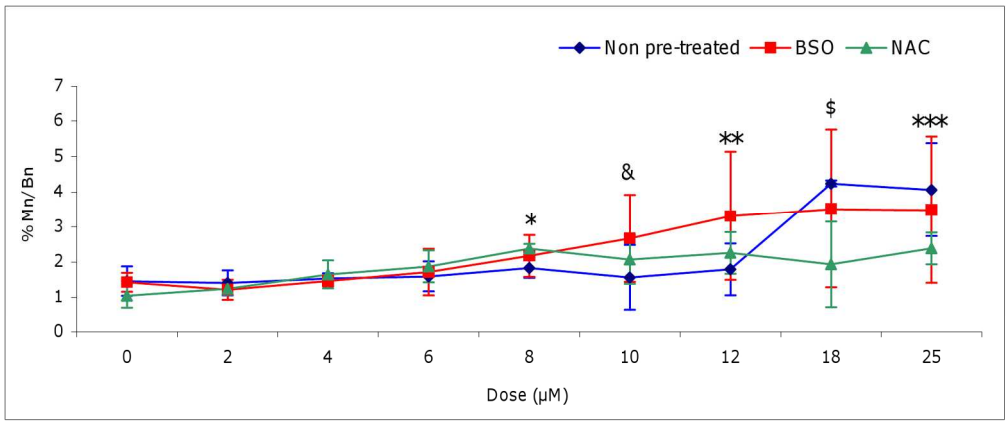

Figure 6. Pro-oxidant dose response following alteration of cellular glutathione antioxidant levels. Effect of BSO (0.5mM) or NAC (2.0mM) pre-treatment on the frequency of hydrogen peroxide (H2O2) induced micronuclei in AHH-1 cells; *: At 8 μM H2O2, first significant increase in micronuclei (MN) frequency above the control in BSO pre- treated cells (p= 0.0008) as determined by T-test. &: At 10uM H2O2, BSO pre- treated cells demonstrated a statistically significant increase in percentage MN as compared to non pre-treated and NAC pre- treated cells ($p<0.001$ and $p< 0.05$, respectively); **: At 12μM H2O2, BSO pre-treated cells showed a statistically significant elevation in MN as compared to non pre- treated cells ($p<0.01$); $: At 18uM H2O2, first statistically significant increase in MN frequency above the control in non pre- treated cells ($p<0.0001$); also, non pre-treated cells exhibited statistically significant higher levels of MN to NAC pre-treated cells ($p<0.001$); ***: At 25uM H2O2, non pre-treated cells had statistically significant higher levels of micronuclei than NAC pre-treated cells ($p<0.01$). Mn/Bn%: percentage of binucleated cells containing one or more micronuclei.
169x70mm (300 x 300 DPI)